Clays and Clay Minerals, Vol. 51, No. 2, 162–167, 2003.

DIFFERENCES IN QUASICRYSTALS OF SMECTITE-CATIONIC SURFACTANT COMPLEXES DUE TO HEAD GROUP STRUCTURE

YUSUKE IMAI*, SATOSHI NISHIMURA, YOSHINARI INUKAI AND HIROSHI TATEYAMA

Institute for Structural and Engineering Materials, National Institute of Advanced Industrial Science and Technology 807-1, Shuku-machi, Tosu, Saga 841-0052, Japan

Abstract—The organoclay quasicrystals formed by exchange reactions of fluoromagnesian smectite (FMS) and two kinds of cationic surfactants were investigated by X-ray diffraction (XRD) of both aqueous suspensions and dried powders. ζ potential measurements were also carried out. The two cationic surfactants employed in this study, dodecyltriphenylphosphonium bromide (C_{12}PBr) and dodecyltrimethylammonium bromide (C_{12}NBr), have the same alkyl chain length but different head group structures. In aqueous suspensions of C_{12}N/FMS, regular stacking with a basal spacing of 2.28 nm was observed within the range 0.4 to 1.0 of the cation exchange capacity (CEC) of the C_{12}N/FMS ratios. The basal spacing was constant in this range. The most intense diffraction for the C_{12}N/FMS suspension was observed at 0.6 CEC, and a further increase in the C_{12}N/FMS ratio resulted in a decline of the diffraction intensity and a slight increase in the peak width. On the other hand, in C_{12}P/FMS suspensions with the surfactant/FMS ratios <0.6 CEC, only weak, broad XRD peaks were observed. With higher C_{12}P/FMS ratios (0.8 and 1.0 CEC), strong diffraction peaks appeared with a basal spacing of 3.20 nm. The difference in the observed basal spacings of C_{12}N/FMS and C_{12}P/FMS tactoids was ~0.9 nm, which did not agree with the difference in the estimated height of the two surfactants (~0.1 nm). These differences of the tactoid structures between C_{12}N/FMS and C_{12}P/FMS suspensions could be explained in terms of the difference in the adsorption manner of the surfactants on the silicate surface and in the size of the surfactant head groups.

Key Words—Adsorption, Dodecyltrimethylammonium Bromide, Dodecyltriphenylphosphonium Bromide, Fluoromagnesian Smectite, Hemimicelle, Intercalation Compounds, Stacking, Tactoids, X-ray Diffraction, Zeta Potential

INTRODUCTION

Intercalation of organic cationic surfactants into layered silicates converts the essentially hydrophilic internal surface of the layered silicates into a hydrophobic one. The surfactant/layered silicate intercalation compounds obtained have been utilized in a wide variety of important applications in various fields, *e.g.* removal of organic pollutants from wastewater (Meier *et al.*, 2001), rheological control agents (Jones, 1983), and polymer nanocomposites (Pinnavaia and Beall, 2000). The structure of the intercalation compounds from alkylammonium salts has been the objective of many studies (Klapyta *et al.*, 2001; Venkataraman and Vasudevan, 2001; Yang *et al.*, 2001). We have investigated the interaction between dodecyltrimethylammonium bromide (C_{12}NBr) and synthetic fluoromagnesian smectite (FMS) in water and their tactoid structures in water by XRD and atomic force microscopy (AFM) (Kuwaharada *et al.*, 2002; Whitby *et al.*, 2001). A regular interstratified structure of the intercalation compounds composed of aliphatic phosphonium salts and fluorohectorite was reported by Ijdo *et al.* (1996) and by Ijido and Pinnavaia (1998, 1999). The intercalation compounds prepared from aromatic phosphonium salts possess a superior thermal stability compared to those from ammonium salts. They have been utilized to improve the fire-retardant property of polymer nanocomposites (Zhu *et al.*, 2001). We have been developing poly(ethylene terephthalate) (PET)/FMS nanocomposites. In order to do this the intercalation compounds formed using ammonium surfactants cannot be employed because of their low thermal stability. The PET/FMS nanocomposites have been successfully prepared by employing the novel triphenylphosphonium surfactant as a compatibilizer (Imai *et al.*, 2002). It is necessary to understand the formation process and the tactoid structure of the triphenylphosphonium surfactants/FMS intercalation compounds to improve the properties of the PET/FMS nanocomposites further. However, a detailed study has not yet been carried out.

In this study, we investigated the formation of the tactoid structure of dodecyltriphenylphosphonium bromide (C_{12}PBr)/FMS intercalation compounds by XRD and ζ potential measurements. The results were compared with those of the C_{12}N/FMS compounds in order to assess the influence of the head group upon the tactoid structure.

EXPERIMENTAL

Materials

Pure FMS was used as the starting material (Tateyama *et al.*, 1992, 1996). This smectite is similar

* E-mail address of corresponding author:
y-imai@aist.go.jp
DOI: 10.1346/CCMN.2003.0510205

Copyright © 2003, The Clay Minerals Society

https://doi.org/10.1346/CCMN.2003.0510205 Published online by Cambridge University Press

in physical and swelling characteristics to a trioctahedral magnesian smectite close to stevensite. The structural formula of FMS is $Na_{0.66}Mg_{2.68}(Si_{3.98}Al_{0.02})O_{10.02}F_{1.96}$ and the unit-cell parameters of FMS are a = 0.524, b = 0.908, c = 0.970 nm, and β = 100º. The CEC of FMS is 1.20 mmol g^{-1}. This material is commercially available as ME-100 from CO-OP Chemical, Co., Ltd., Japan. Dodecyltrimethylammonium bromide ($C_{12}NBr$) was obtained from Tokyo Kasei Co., Ltd., Japan, and used as received. Dodecyltriphenylphosphonium bromide ($C_{12}PBr$) was synthesized from 1-bromododecane and triphenylphosphine by heating an equimolar mixture at 100ºC for 12 h. The resulting solidified product was purified by recrystallization from acetone/methyl *tert*-butyl ether.

Sample preparation

A two-stage mixing process of FMS and water was employed to achieve complete exfoliation of the FMS in water. 8 g of FMS were mixed with 92 g of deionized water for 2 min in a blender to obtain a uniform gel of the clay and water. Then, 1.25 g of the clay gel (containing 0.10 g of FMS) and 8.85 g of deionized water were mixed and stirred at room temperature for 1 h to obtain a 1 wt.% dispersion of FMS in water. The surfactants were dissolved in 90 g of deionized water and an aqueous dispersion of FMS was added. The resulting suspension was stirred at 25ºC for at least 48 h. The surfactant-to-FMS ratios (surfactant/FMS) were varied from 0.12 to 2.4 CEC. A portion of the suspension was centrifuged at 6,000 rpm for 20 min and the supernatant was used for the UV absorption measurements. The sediment was dried under vacuum at room temperature and used for the powder XRD measurements.

X-ray diffraction data

The instrumentation for the XRD analysis of the suspension is shown schematically in Figure 1 (Tateyama *et al.*, 1997). A sample was poured into a sample cell the bottom of which was covered by a 2.5 μm thick Mylar film (Chemplex X-ray film Mylar). The sample cell was then placed on the stainless steel holder of the XRD instrument. The sample cell assembly was mounted on the axis of a Philips APD X'Pert diffractometer. X-ray beams were diffracted from the bottom plane of the sample holder. The XRD and powder XRD data were collected using CuKα radiation from 1 to 10º2θ at a step size of 0.05º and a measuring time of 20 s per step.

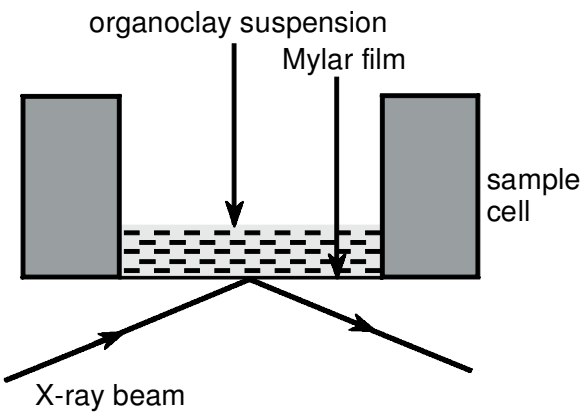


Figure 1. Schematic drawing of the instrumentation for the XRD analysis of the suspensions.

UV absorption measurements

The concentration of $C_{12}P$ in the supernatant liquid was determined by UV absorption measurements using a Shimadzu UV-1600 spectrophotometer. The molar absorptivity of $C_{12}P$ in water is 2,600 cm^{-1} mol^{-1} dm^3 at 275 nm and 3,200 cm^{-1} mol^{-1} dm^3 at 267 nm.

Electrophoretic measurements

The ζ potential of FMS was measured on a Penkem system 3000. A small amount of FMS (1 mg) obtained after centrifugation was redispersed by ultrasonic vibration in 50 cm^3 of supernatant liquid, which had the same surfactant concentration as the suspension. The suspension was adjusted to ~pH 5 with aqueous HCl. The ζ potential was calculated using the Helmholtz-Smoluchowski equation.

Structure optimization

The optimization of the structure of the surfactants was carried out using the geometry optimization capability of the PC GAMESS program (version 6.2) with the STO-3G basis sets (Schmidt *et al.*, 1993).

RESULTS

Figure 2 shows the ζ potential of FMS as a function of the surfactant/FMS ratio. Both $C_{12}P$/FMS and

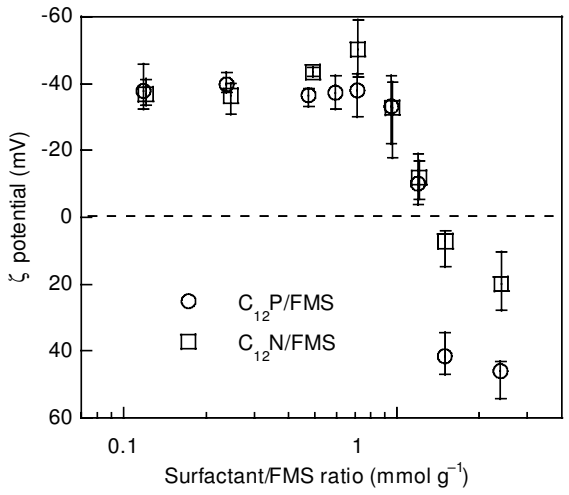


Figure 2. ζ potential of FMS as a function of the surfactant/FMS ratio.

https://doi.org/10.1346/CCMN.2003.0510205 Published online by Cambridge University Press

C_{12}N/FMS showed similar profiles. The ζ potential was almost constant in the region where the surfactant/FMS ratio was not more than 0.6 CEC. For larger ratios, the absolute value of the ζ potential began to decrease and the isoelectric point occurred at a surfactant/FMS ratio of ~1.0 CEC.

In the UV absorption measurements of the supernatants of the centrifuged C_{12}P/FMS suspensions, the 267 and 275 nm absorption of C_{12}P was not observed when the C_{12}P/FMS ratio was below the CEC. These results indicate that C_{12}P adsorption to FMS was almost quantitative in this range. In a previous study (Nishimura *et al.*, 1995), it was confirmed that C_{12}N was completely adsorbed on a mica surface in the concentration range employed in this study.

The XRD patterns of aqueous suspensions and dried powders of the C_{12}N/FMS and C_{12}P/FMS organoclays are shown in Figures 3 and 4, respectively. For the C_{12}N/FMS suspensions, the 00*l* diffraction peaks were clearly observed for surfactant/FMS ratios >0.4 CEC. On the other hand, only weak broad peaks were observed with the C_{12}P/FMS suspensions <0.6 CEC, whereas strong diffraction peaks appeared above 0.8 CEC. The positions of the strong diffraction peaks in both organoclay suspensions did not change with the surfactant/FMS ratios. For C_{12}N/FMS, the 00*l* series appeared at 2.30 and 1.13 nm with an average basal spacing of 2.28 nm. For C_{12}P/FMS, the 00*l* series appeared at 3.21 and 1.59 nm with an average basal spacing of 3.20 nm. The most intense diffraction for the C_{12}N/FMS suspension was observed at 0.6 CEC. A further increase in the C_{12}N/FMS ratio resulted in a decline of the diffraction intensity and a slight increase in the peak width.

In the dried-powder XRD patterns, all samples with surfactant/FMS ratios from 0.2 to 1.0 CEC produced 00*l* reflections. The range of basal spacings in the dried powders was narrower than that in the suspensions. In the C_{12}N/FMS powders, the basal spacing increased from 1.32 to 1.61 nm with an increase in the C_{12}N/FMS ratio from 0.2 to 0.6 CEC, while it became constant (1.79 nm) between 0.8 and 1.0 CEC. The diffraction peaks were broad with small C_{12}N/FMS ratios, while the sharp diffraction peaks comparable to those in the suspensions were observed along with higher ratios. The general tendency was substantially the same for the C_{12}P/FMS powders. For the 0.8 CEC C_{12}P/FMS powder, the intensity of the broad peak at 1.92 nm was reduced and sharp 00*l* diffraction peaks appeared at 2.60 and 1.34 nm. The peaks of the 1.0 CEC C_{12}P/FMS powder were as sharp as those in the suspensions.

Figure 5a,b illustrates the optimized structures of C_{12}N and C_{12}P with the dodecyl group in the all-*trans* conformation. Assuming that the three methyl groups of C_{12}N and the three phenyl groups of C_{12}P face the FMS

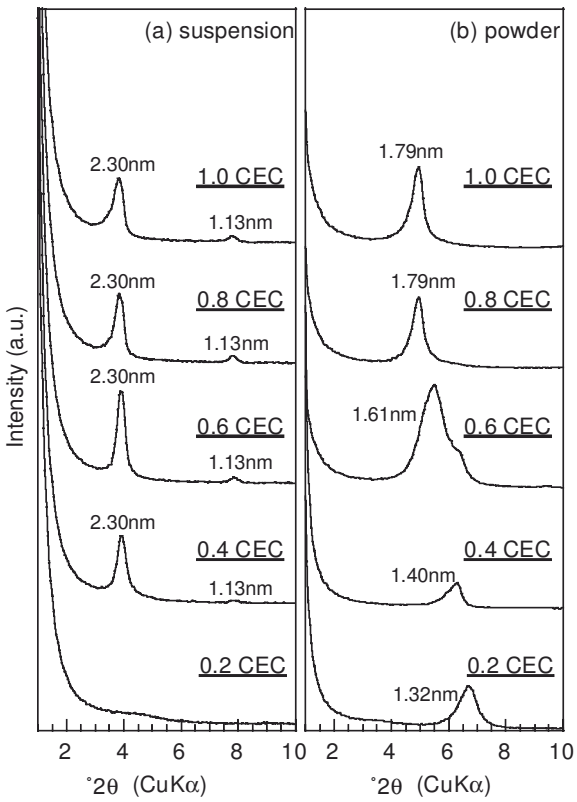


Figure 3. XRD patterns of C_{12}N/FMS tactoids in suspensions (a) and as dried powders (b).

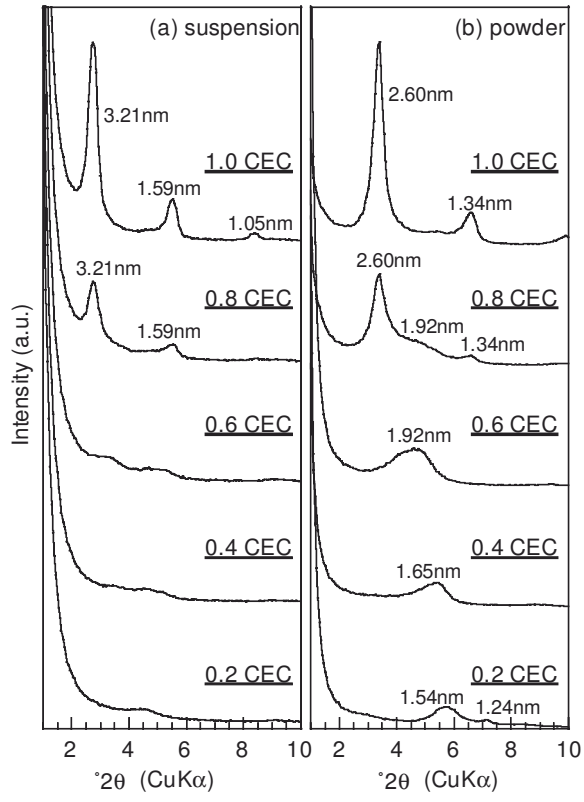


Figure 4. XRD patterns of C_{12}P/FMS tactoids in suspensions (a) and as dried powders (b).

https://doi.org/10.1346/CCMN.2003.0510205 Published online by Cambridge University Press

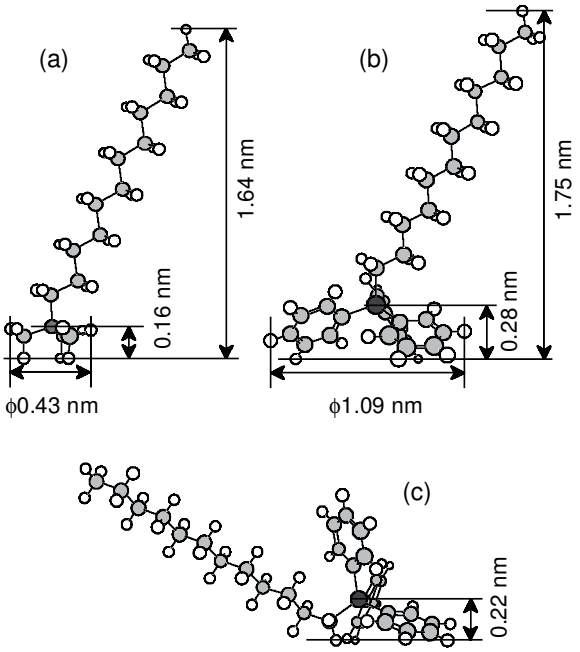


Figure 5. The calculated model structure of (a) $C_{12}N$ in all-*trans* conformation, (b) $C_{12}P$ in all-*trans* conformation, and (c) one possible conformation of $C_{12}P$ adsorbed on the FMS surface.

plane, the vertical distances of the terminal of the alkyl chain from the FMS plane (the height of the molecules) were estimated to be 1.64 and 1.75 nm for $C_{12}N$ and $C_{12}P$, respectively. The diameters of the head groups were estimated to be 0.43 and 1.09 nm for $C_{12}N$ and $C_{12}P$, respectively.

DISCUSSION

From the results of the UV absorption and ζ potential measurements, it was confirmed that both $C_{12}N$ and $C_{12}P$ were almost completely adsorbed on FMS. However, there were some distinct differences between these compounds. The regular stacking of FMS in an aqueous suspension took place at the different surfactant/FMS ratios. Moreover, the observed difference in the basal spacings of the tactoid structures of the $C_{12}N$/FMS and $C_{12}P$/FMS organoclays in the aqueous suspension was ~0.9 nm. This is very different from the estimated difference in the height of the molecules (~0.1 nm). Hereafter, we intend to explain the reasons for such differences.

$C_{12}N$/FMS compounds

In aqueous suspensions, FMS is completely delaminated and randomly dispersed (Kuwaharada *et al.*, 2002). During the mixing process of the FMS suspension with the $C_{12}N$ solution, $C_{12}N$ adsorbs on FMS, and the surface of FMS becomes more hydrophobic. The stacking of FMS then occurs with a finite particle distance and the tactoid is formed. Both adsorbed $C_{12}N$ and H_2O molecules exist in the interlayer region of the tactoid structure. It is considered that the distance between the stacked silicate layers reflects the orientation and conformation of the hydrocarbon chain of the adsorbed $C_{12}N$. From the fact that the basal spacings of the $C_{12}N$/FMS tactoids were constant within the range of 0.4 to 1.0 CEC of the $C_{12}N$/FMS ratios, it is suggested that the orientation and conformation of the adsorbed $C_{12}N$ do not vary significantly in this range. It has been reported that $C_{12}N$ molecules aggregate to form the so-called hemimicelle structure at the mica-water interface much below its bulk critical micelle concentration due to lateral hydrophobic interactions between the hydrocarbon chains (Hough and Rendall, 1983; Nishimura *et al.*, 1995). It is likely that the orientation and conformation of $C_{12}N$ forming such hemimicelles are mainly governed by the local concentration of $C_{12}N$ on the FMS surface, and almost independent of the $C_{12}N$/FMS ratios. Therefore, the basal spacings of the $C_{12}N$/FMS tactoids can be explained by the orientation and conformation of the $C_{12}N$ hemimicelle. The observed value of the basal spacing (2.28 nm) was slightly smaller than the sum of the silicate layer thickness (0.96 nm) and $C_{12}N$ height (1.64 nm). This difference suggests that the hydrocarbon chain of $C_{12}N$ bends and tilts to some extent. It is difficult to determine at present whether $C_{12}N$ forms a one- or two-molecular layer in the interlayer region. However, considering the constant basal spacings in the range of 0.4 to 1.0 CEC of the $C_{12}N$/FMS ratios, the one-molecular layer structure is more likely. This model can also be supported by the 1.01 nm^2 adsorption site area on the FMS surface, and the 0.43 nm diameter of the trimethylammonium group.

The ζ potentials of $C_{12}N$/FMS were almost constant below 0.6 CEC. This indicates that adsorbed $C_{12}N$ mainly exists in the interlayer region of the tactoids. This is reasonable in view of the hydrophobicity of $C_{12}N$. The most intense diffraction observed at 0.6 CEC indicates the most regular stacking. This can be attributed to the sufficient condensation of $C_{12}N$ in the interlayer region to achieve a regular stacking. An increase in the $C_{12}N$/FMS ratio probably inhibits rearrangement of the silicate layers and thus the decline of the stacking regularity.

The increase in the basal spacings of the dried powders with increasing $C_{12}N$/FMS ratios is consistent with an increase in the amount of adsorbed surfactants. When the $C_{12}N$/FMS ratios were 0.4 and 0.6, the diffraction peaks of the dried powders were broader than those of the suspensions. The removal of H_2O molecules from the interlayer region during drying results in a decrease in the basal spacing, and at the same time, compression of the $C_{12}N$ hemimicelle. This would cause the variation in the orientation and conformation of the $C_{12}N$ hemimicelle, and consequently, the decreased stacking regularity. However, if the $C_{12}N$/FMS ratios are sufficiently large, the $C_{12}N$

https://doi.org/10.1346/CCMN.2003.0510205 Published online by Cambridge University Press

hemimicelle can act as a stable pillar, and the stacking of the dried powder becomes more regular.

C_{12}P/FMS compounds

In the case of C_{12}P/FMS, regular stacking in the suspension was only observed with relatively high C_{12}P/FMS ratios. The observed basal spacing (3.20 nm) was ~0.9 nm greater than that of C_{12}N/FMS (2.28 nm). This does not agree with the difference in the estimated height of the two surfactants (~0.1 nm). Therefore, there must be a certain difference in the stacking mechanism between C_{12}N/FMS and C_{12}P/FMS. There are two probable causes; one concerns the adsorption manner of C_{12}P on FMS. The cationic surfactants and the anionic adsorption sites of FMS attract each other via an electrostatic force. It is thermally more stable with a shorter distance between the charges. For C_{12}N, the distance becomes shortest when the three methyl groups face the surface. On the contrary, because the phenyl group is considerably larger than the methyl group, more than one conformation is possible for C_{12}P. One is that the three phenyl groups face the surface (Figure 5b). The other possible conformation is that the two phenyl groups and the alkyl group face the surface (Figure 5c). The adsorbed C_{12}P molecules can aggregate due to lateral hydrophobic interactions. However, the various adsorption manners would inhibit the effective interaction between the hydrocarbon chains, and hence would restrict the formation of the ordered hemimicelle structure. These assumptions can explain the lack of the regular stackings in the range of 0.2 to 0.6 CEC of the C_{12}P/FMS ratios in the suspensions. In other words, the broadening of the diffraction peaks of the suspensions of C_{12}P/FMS as compared to C_{12}N/FMS indicates the difficulty in forming the regularly stacked tactoids in C_{12}P/FMS.

The difference in the size of the surfactant head groups would be a second possible reason for the different stacking behavior. The regular stacking of FMS was observed as the C_{12}P/FMS ratios increased to more than 0.8 CEC in the suspensions. The observed basal spacings (3.20 nm) were larger than the sum of the silicate layer thickness (0.96 nm) and the height of C_{12}P (1.75 nm). This implies the possible formation of a two-molecular layer of C_{12}P in the interlayer region. The diameter of the triphenylphosphonium group (1.09 nm) is greater than that of the trimethylammonium group (0.43 nm), and the area is somewhat larger than that of the adsorption site. Consequently, it is considered that a two-molecular layer is formed in the interlayer region of the C_{12}P/FMS tactoids, unlike C_{12}N/FMS. When the C_{12}P/FMS ratio was 1.0 CEC, sharp 00*l* reflections were observed indicating regular stacking. This result implies that as the C_{12}P concentration increases, C_{12}P tends to take a specific conformation, which would lead to ordered stacking. For a C_{12}P/FMS ratio of 1.0 CEC, regular stacking of tactoids is maintained even after drying.

Although both C_{12}P and C_{12}N are cationic surfactants with the same alkyl chain length, there are some differences in the stacking structures and the formation process of the tactoids with FMS. In order to explain these differences more clearly, it is considered necessary to evaluate the lateral interaction between the surfactant molecules adsorbed on the silicate layer. The study on this issue is now in progress.

CONCLUSIONS

The formation process and the stacking structure of the C_{12}P/FMS intercalation compounds were investigated by XRD of the suspensions and powders, as well as ζ potential measurements. The results were then compared with those of the C_{12}N/FMS compounds. It was found that regular stacking of FMS in an aqueous suspension took place at different surfactant/FMS ratios. The differences in the basal spacings of the tactoid structures in both aqueous suspensions disagreed with the estimated difference in the height of the surfactants. These differences could be attributed to differences in the adsorption manner of the surfactants on the silicate surface and on the size of the surfactant head groups.

ACKNOWLEDGMENTS

This work was supported in part by the Special Coordination Funds for Promoting Science and Technology (Fluidity Promoting Research System) from the Ministry of Education, Culture, Sports, Science and Technology, Japan. We would like to thank Dr Toshiaki Koga, Dr Hiroaki Noma and Dr Yoshio Adachi, AIST Kyushu, for helpful discussions.

REFERENCES

Hough, D.B. and Rendall, H.M. (1983) Adsorption of ionic surfactants. Pp. 247–319 in: *Adsorption from Solution at the Solid/Liquid Interface* (G.D. Parfitt and C.H. Rochester, editors). Academic Press, Inc., London.

Ijdo, W.L., Lee, T. and Pinnavaia, T.J. (1996) Regularly interstratified layered silicate heterostructures: precursors to pillared rectorite-like intercalates. *Advanced Materials*, **8**, 79–83.

Ijdo, W.L. and Pinnavaia, T.J. (1998) Staging of organic and inorganic gallery cations in layered silicate heterostructures. *Journal of Solid State Chemistry*, **139**, 281–289.

Ijdo, W.L. and Pinnavaia, T.J. (1999) Solid solution formation in amphiphilic organic-inorganic clay heterostructures. *Chemistry of Materials*, **11**, 3227–3231.

Imai, Y., Nishimura, S., Abe, E., Tateyama, H., Abiko, A., Yamaguchi, A., Aoyama, T. and Taguchi, H. (2002) High-modulus poly(ethylene terephthalate)/expandable fluorine mica nanocomposites with a novel reactive compatibilizer. *Chemistry of Materials*, **14**, 477–479.

Jones, T.R. (1983) The properties and uses of clays which swell in organic solvents. *Clay Minerals*, **18**, 399–410.

Klapyta, Z., Fujita, T. and Iyi, N. (2001) Adsorption of dodecyl- and octadecyltrimethylammonium ions on a smectite and synthetic micas. *Applied Clay Science*, **19**, 5–10.

Kuwaharada, S., Tateyama, H., Nishimura, S. and Hirosue, H. (2002) Smectite quasicrystals in aqueous solutions as a

https://doi.org/10.1346/CCMN.2003.0510205 Published online by Cambridge University Press

function of cationic surfactant concentration. *Clays and Clay Minerals*, **50**, 18–24.

Meier, L.P., Nueesch, R. and Madsen, F.T. (2001) Organic pillared clays. *Journal of Colloid and Interface Science*, **238**, 24–32.

Nishimura, S., Scales, P.J., Biggs, S.R. and Healy, T.W. (1995) AFM studies of amine surfactant hemimicelle structures at the mica–water interface. *Colloids and Surfaces A*, **103**, 289–298.

Pinnavaia, T.J., and Beall, G.W., editors (2000) *Polymer–Clay Nanocomposites*. John Wiley & Sons Ltd., Chichester, England.

Schmidt, M.W., Baldridge, K.K., Boatz, J.A., Elbert, S.T., Gordon, M.S., Jensen, J.J., Koseki, S., Matsunaga, N., Nguyen, K.A., Su, S., Windus, T.L., Dupuis, M. and Montgomery, J.A. (1993) General atomic and molecular electronic-structure system. *Journal of Computational Chemistry*, **14**, 1347–1363; Granovsky, A.A. www: http://classic.chem.msu.su/gran/gamess/index.html.

Tateyama, H., Nishimura, S., Tsunematsu, K., Jinnai, K., Adachi, Y. and Kimura, M. (1992) Synthesis of expandable fluorine mica from talc. *Clays and Clay Minerals*, **40**, 180–185.

Tateyama, H., Tsunematsu, K., Noma, H. and Adachi, Y. (1996) Formation of expandable fluorine mica from talc using the intercalation procedure. *Journal of the American Ceramic Society*, **79**, 3321–3324.

Tateyama, H., Scales, P.J., Ooi, M., Nishimura, S., Rees, K. and Healy, T.W. (1997) X-ray diffraction and rheology study of highly ordered clay platelet alignment in aqueous solutions of sodium tripolyphosphate. *Langmuir*, **13**, 2440–2446.

Venkataraman, N.V. and Vasudevan, S. (2001) Conformation of methylene chains in an intercalated surfactant bilayer. *Journal of Physical Chemistry B*, **105**, 1805–1812.

Whitby, C.P., Scales, P.J., Grieser, F., Healy, T.W., Nishimura, S. and Tateyama, H. (2001) The adsorption of dodecyltrimethylammonium bromide on mica in aqueous solution studied by X-ray diffraction and atomic force microscopy. *Journal of Colloid and Interface Science*, **235**, 350–357.

Yang, J.-H., Han, Y.-S., Choy, J.-H. and Tateyama, H. (2001) Intercalation of alkylammonium cations into expandable fluorine mica and its application for the evaluation of heterogeneous charge distribution. *Journal of Materials Chemistry*, **11**, 1305–1312.

Zhu, J., Morgan, A.B., Lamelas, F.J. and Wilkie, C.A. (2001) Fire properties of polystyrene–clay nanocomposites. *Chemistry of Materials*, **13**, 3774–3780.

(*Received 29 April 2002; revised 21 October 2002; Ms. 652; A.E. William F. Jaynes*)

https://doi.org/10.1346/CCMN.2003.0510205 Published online by Cambridge University Press